Stem Cell Reports
Article
ISSCR
OPEN ACCESS

Amyloid β Is Not the Major Factor Accounting for Impaired Adult Hippocampal Neurogenesis in Mice Overexpressing Amyloid Precursor Protein

Hongyu Pan,[1] Dongpi Wang,[1] Xiaoqin Zhang,[1] Dongming Zhou,[1] Heng Zhang,[1] Qi Qian,[2] Xiao He,[1] Zhaoling Liu,[1] Yunjin Liu,[1] Tingting Zheng,[3] Ling Zhang,[1] Mingkai Wang,[1] and Binggui Sun[1,*]
[1]Department of Neurobiology, School of Basic Medical Sciences, Key Laboratory of Medical Neurobiology (Ministry of Health of China), Key Laboratory of Neurobiology of Zhejiang Province
[2]Department of Neurology, Brain Medical Center, First Affiliated Hospital
[3]Department of Neurology, Second Affiliated Hospital
Zhejiang University School of Medicine, Hangzhou, Zhejiang Province 310058, China
*Correspondence: bsun@zju.edu.cn
http://dx.doi.org/10.1016/j.stemcr.2016.08.019

SUMMARY

Adult hippocampal neurogenesis was impaired in several Alzheimer's disease models overexpressing mutant human amyloid precursor protein (hAPP). However, the effects of wild-type hAPP on adult neurogenesis and whether the impaired adult hippocampal neurogenesis was caused by amyloid β (Aβ) or APP remained unclear. Here, we found that neurogenesis was impaired in the dentate gyrus (DG) of adult mice overexpressing wild-type hAPP (hAPP-I5) compared with controls. However, the adult hippocampal neurogenesis was more severely impaired in hAPP-I5 than that in hAPP-J20 mice, which express similar levels of hAPP mRNA but much higher levels of Aβ. Furthermore, reducing Aβ levels did not affect the number of doublecortin-positive cells in the DG of hAPP-J20 mice. Our results suggested that hAPP was more likely an important factor inhibiting adult neurogenesis, and Aβ was not the major factor affecting neurogenesis in the adult hippocampus of hAPP mice.

INTRODUCTION

Neurogenesis occurs in the subgranular zone (SGZ) of the dentate gyrus (DG) throughout life in the adult brain of most mammals including human beings (Bond et al., 2015; Eriksson et al., 1998; Spalding et al., 2013). Newly generated neurons can be integrated into the pre-existing neural circuits (Ge et al., 2007; Lledo et al., 2006; Restivo et al., 2015; Sultan et al., 2015; Tashiro et al., 2006a; van Praag et al., 2002). Although the physiological roles of newborn neurons are not fully understood, many studies indicated that they were involved in the hippocampus-dependent functions such as learning and memory, mood regulation, and pattern separation (Christian et al., 2014; Clelland et al., 2009; Deng et al., 2010; Kang et al., 2016; Sahay et al., 2011a, 2011b; Shors et al., 2001). The process of neurogenesis in the adult brain consists of several stages including proliferation, differentiation, migration, survival, axonal and dendritic targeting, and synaptic integration (Ehninger and Kempermann, 2008). Intense efforts were conducted in the past several years to dissect how the different stages of neurogenesis were regulated (Bond et al., 2015). Physical activities such as exercise and an enriched environment can prompt neurogenesis (Marlatt et al., 2013; Nilsson et al., 1999; Valero et al., 2011; van Praag et al., 1999). Stress, aging, and neurological disorders, however, may inhibit neurogenesis (Richetin et al., 2015; Winner et al., 2011; Yun et al., 2010; Zhao et al., 2008).

Alzheimer's disease (AD) is the most common neurodegenerative disorder. The pathological hallmarks of AD include extracellular amyloid plaques consisting mainly of Aβ42, and intracellular neurofibrillary tangles comprising mainly hyperphosphorylated tau (Serrano-Pozo et al., 2011). Previous studies reported that adult hippocampal neurogenesis was affected in AD patients. However, results from different groups were not consistent (Boekhoorn et al., 2006; Jin et al., 2004; Li et al., 2008). On the other hand, it was nearly impossible to investigate systematically the effects of AD on different stages of adult neurogenesis by using samples from AD patients. Therefore, animal models simulating key pathological features of AD provided invaluable tools to study the effects of different factors involved in AD on adult neurogenesis (Epis et al., 2010). Transgenic mice overexpressing human amyloid precursor proteins (hAPP) are common animal models of AD. Although data from different studies were still controversial, most experimental results indicated that adult hippocampal neurogenesis was adversely disturbed in mice with hAPP overexpression (Chuang, 2010; Donovan et al., 2006; Haughey et al., 2002). However, hAPP-overexpressing mice contained higher levels of both hAPP and amyloid β (Aβ) in the brain compared with nontransgenic controls (Mucke et al., 2000). It remained unknown, therefore, whether a high level of hAPP or Aβ was the major factor accounting for impaired adult neurogenesis in these models. Besides, mice overexpressing mutant hAPP were

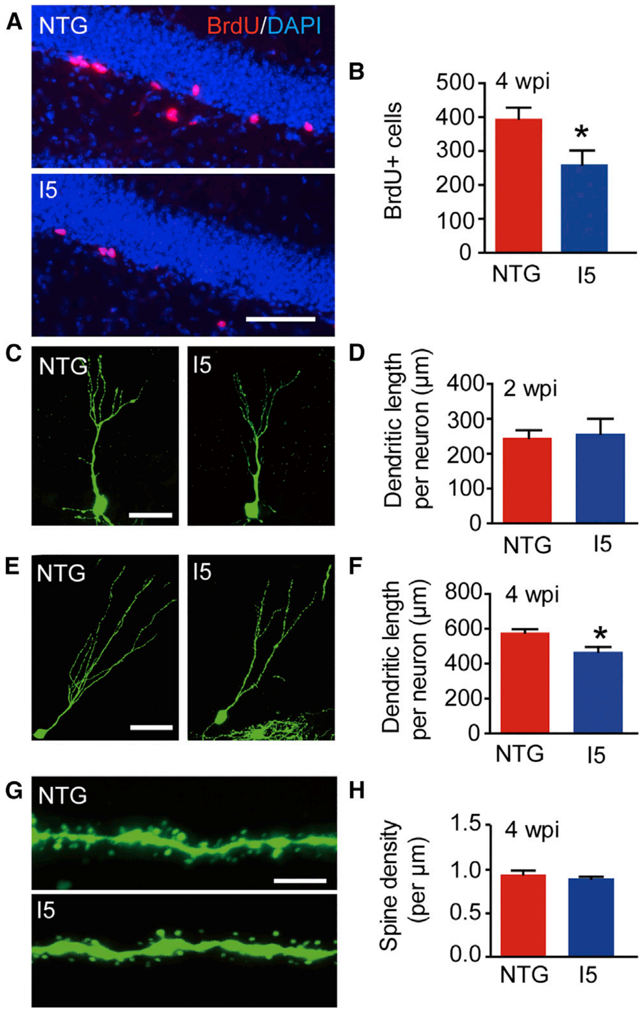

Figure 1. Wild-Type hAPP Overexpression Reduced the Number and Impaired the Morphology of Newborn Neurons

(A) Representative photomicrographs of immunohistochemical staining for BrdU in hAPP-I5 and nontransgenic controls (2.5 months old) at 28 days after the last BrdU injection. BrdU staining is shown as red; nuclei were labeled by DAPI shown as blue. Scale bar, 100 μm.

(B) Quantification of BrdU-positive cells in the SGZ of dentate gyrus in hAPP-I5 mice (n = 6, 3 female and 3 male) and nontransgenic control mice (n = 6, 3 female and 3 male). *$p < 0.05$ (unpaired t test); values represent mean ± SEM.

(C, E, and G) Representative photomicrographs of dendrites of newborn neurons labeled by retrovirus-GFP at 2 weeks post injection (wpi) (C) and 4 wpi (E), and spine densities of newborn neurons at 4 weeks old (G) in hAPP-I5 and nontransgenic control mice. Scale bars, 30 μm (C), 50 μm (E), and 5 μm (G).

(D, F, and H) Quantification of total dendritic length per newborn neuron at 2 wpi (n = 5, female) (D), 4 wpi (n = 3 for control mice, n = 6 for hAPP-I5 mice, all female mice) (F), and spine densities at 4 wpi (n = 4 for control mice, n = 6 for hAPP-I5 mice, all female mice) (H) in hAPP-I5 and nontransgenic control mice. *$p < 0.05$ (unpaired t test); values represent mean ± SEM.

See also Figure S1.

used in most of the studies. The effects of wild-type hAPP, which is harbored in most sporadic AD patients, on adult neurogenesis were far from clear.

In the present study, we investigated adult hippocampal neurogenesis in hAPP-I5 mice that overexpressed wild-type hAPP in neurons driven by platelet-derived growth factor (PDGF) β-chain promoter. Furthermore, we compared adult neurogenesis in hAPP-I5 and hAPP-J20 mice. These two lines of mice expressed similar levels of hAPP mRNA but very different levels of Aβ in the brain (Mucke et al., 2000). We found that adult hippocampal neurogenesis was impaired in hAPP-I5 mice. More interestingly, the degree of impairment of neurogenesis was more prominent in hAPP-I5 mice compared with that of hAPP-J20 mice, and downregulating Aβ levels did not affect the number of newborn neurons in hAPP-J20 mice, suggesting that Aβ was not the major factor accounting for impaired adult hippocampal neurogenesis.

RESULTS

Adult Hippocampal Neurogenesis Was Impaired in hAPP-I5 Mice

To test whether adult neurogenesis was affected in hAPP-I5 mice, we injected bromodeoxyuridine (BrdU) intraperitoneally into 2.5-month-old hAPP-I5 and nontransgenic control mice. Four weeks later, mice were perfused and brain sections were analyzed by free-floating immunofluorescence staining using anti-BrdU antibody. The number of $BrdU^+$ cells was significantly reduced in the hippocampus of hAPP-I5 mice compared with that of nontransgenic control mice (Figures 1A and 1B). Because hippocampal neural stem cells can differentiate into neurons and astrocytes, brain slices from mice injected with BrdU were then co-immunostained with antibodies against BrdU and NeuN, a mature neuronal marker. The number of BrdU and NeuN double-positive cells was also dramatically reduced in hAPP-I5 mice compared with that of control mice (Figures S1A and S1B). However, the ratio of $BrdU^+/NeuN^+$ to total $BrdU^+$ cells was similar between hAPP-I5 and control mice (Figure S1C), suggesting that the differentiation of neural stem cells to neurons was not affected in hAPP-I5 mice. Taken together, these data indicated that adult hippocampal neurogenesis was impaired in hAPP-I5 mice.

To further examine whether the development of newborn neurons was affected in the hippocampus of adult hAPP-I5 mice, we stereotactically injected a murine Moloney leukemia virus-based retroviral vector expressing EGFP (Zhao et al., 2006) into the DG to label newly generated neurons. Retrovirus labeled only dividing cells (Zhao et al., 2006). Therefore, the day of the injection marked the birth date of neurons. We analyzed GFP-labeled

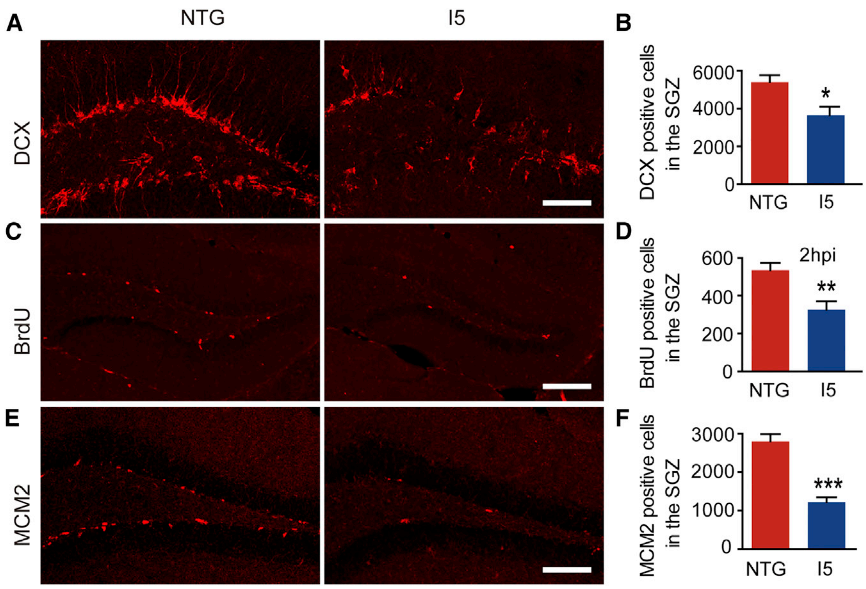

Figure 2. Wild-Type hAPP Overexpression Decreased the Number of Immature Neurons and Proliferation of Neural Progenitor Cells

(A) Representative photomicrographs of DCX^+ immature neurons in the DG of hAPP-I5 and nontransgenic control mice (2.5 months old). Scale bar, 100 μm.

(B) Quantification of DCX^+ immature neurons in hAPP-I5 mice (n = 7, 4 female and 3 male) and nontransgenic controls (n = 6, 3 male and 3 female). *$p < 0.05$ (unpaired t test); values represent mean ± SEM.

(C) Representative photomicrographs of immunostaining for BrdU in hAPP-I5 mice and nontransgenic control mice (2.5 months old) at 2 hr after BrdU injection. Scale bar, 200 μm.

(D) Quantification of $BrdU^+$ cells in the DG of hAPP-I5 mice (n = 5, 3 female and 2 male) and nontransgenic controls (n = 5, 3 female and 2 male). **$p < 0.01$ (unpaired t test); values represent mean ± SEM.

(E) Representative photomicrographs of $MCM2^+$ neural progenitors in 2.5-month-old hAPP-I5 and nontransgenic controls. Scale bar, 100 μm.

(F) Quantification of $MCM2^+$ cells in the DG of hAPP-I5 mice (n = 5, 3 female and 2 male) and nontransgenic controls (n = 8, 5 female and 3 male). ***$p < 0.001$ (unpaired t test); values represent mean ± SEM.

newborn neurons at 14 and 28 days post infection (dpi) by confocal microscopy. At 14 dpi, the newborn neurons were immature. The cell bodies were located in the SGZ, and their dendritic processes extended into the granule cell layer and reached the inner molecular layer. No spines were observed on the dendritic shafts. We measured the dendritic length of GFP-labeled immature neurons at this developmental stage. There was no difference regarding the dendritic length of new neurons between hAPP-I5 and control mice (Figures 1C and 1D). At 28 dpi, the dendritic arborization of newly generated neurons appeared more elaborated than that at 14 dpi, and their processes grew into the molecular layer with many of them reaching the edge of the molecular layer. Spines were frequently observed on the dendritic branches at this stage. We measured the spine density and dendritic length of newborn neurons. Although the spine densities were similar (Figures 1G and 1H), the dendrites of newborn neurons from hAPP-I5 were significantly shorter in comparison with control mice (Figures 1E and 1F). These data further demonstrated that adult neurogenesis was impaired in the hippocampus of hAPP-I5 mice.

Neural Progenitor Cell Proliferation and the Number of Immature Newborn Neurons Decreased in the Adult Hippocampus of hAPP-I5 Mice

The developmental process of newborn neurons in the adult hippocampus includes different stages (Ehninger and Kempermann, 2008). To determine whether earlier developmental stages of newborn neurons were affected, we quantified the doublecortin (DCX)-positive immature neurons in the DG of hAPP-I5 and nontransgenic control mice. We found that DCX-positive neurons were much fewer in number in the DG of hAPP-I5 mice than in the DG of control mice (Figures 2A and 2B). We then injected BrdU intraperitoneally into 2.5-month-old hAPP-I5 and nontransgenic control mice. Neural progenitor cell proliferation was examined at 2 hr after BrdU injection by immunostaining using anti-BrdU antibody. Fewer proliferating cells were observed in the SGZ of hAPP-I5 mice than in nontransgenic control mice (Figures 2C and 2D). To validate this observation, we perfused a different cohort of mice and stained the brain slices with an antibody against MCM2 (minichromosome maintenance type 2), a marker for proliferation. Similarly, the number of MCM2-positive cells was significantly decreased in the DG of hAPP-I5 mice (Figures 2E and 2F). These results demonstrated that neural progenitor cell proliferation and the number of immature newborn neurons decreased in the adult hippocampus of hAPP-I5 mice.

Adult Neurogenesis Was More Significantly Affected in the DG of hAPP-I5 Mice Than in the DG of hAPP-J20 Mice

Adult hippocampal neurogenesis was impaired in hAPP-J20 mice (Sun et al., 2009), a line of transgenic mice

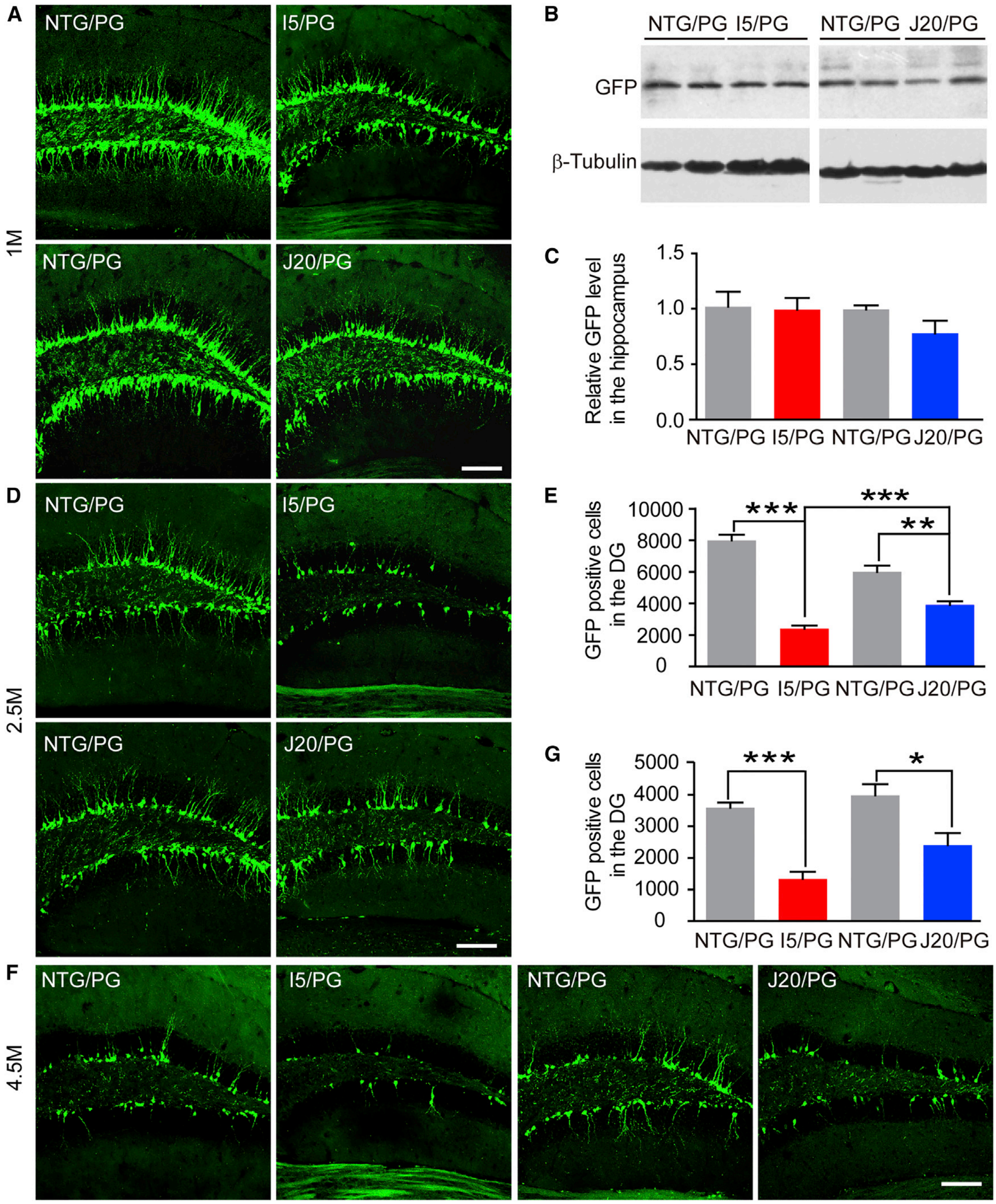

Figure 3. Adult-Born Immature Neurons Labeled via POMC-GFP Mice Numbered Fewer in the DG of hAPP-I5 Mice Than in the DG of hAPP-J20 Mice

(A) Representative photomicrographs of GFP^+ immature neurons in the DG of 1-month-old hAPP-I5/POMC-GFP and hAPP-J20/POMC-GFP mice and their age-matched controls. PG, POMC-GFP; I5/PG, hAPP-I5/POMC-GFP; J20/PG, hAPP-J20/POMC-GFP. Scale bar, 100 μm.

(B) Western blotting bands of GFP expression in 1-month-old hAPP/POMC-GFP mice and age-matched controls. β-Tubulin was used as loading control.

(C) Quantification of western blots showed no significant changes of GFP expression in both hAPP-I5/POMC-GFP (n = 4, 2 male and 2 female) and hAPP-J20/POMC-GFP mice (n = 3, 2 male and 1 female) compared with their controls (n = 3, 2 male and 1 female). One-way ANOVA with Newman-Keuls post hoc test; values represent mean ± SEM.

(legend continued on next page)

overexpressing mutant human APP in neurons driven by the PDGF β-chain promoter. Levels of both hAPP and Aβ were higher in the brain of hAPP-J20 mice in comparison with nontransgenic control mice. Therefore, it was not clear whether the impaired neurogenesis was due to overexpressed hAPP or Aβ. To address this question, we compared adult hippocampal neurogenesis in the DG between hAPP-J20 and hAPP-I5 mice. These two lines of mice expressed similar levels of hAPP mRNA but very different levels of Aβ (Mucke et al., 2000).

To compare the adult hippocampal neurogenesis between hAPP-I5 and hAPP-J20 mice, we took advantage of pro-opiomelanocortin (POMC)-GFP mice, a line of transgenic mice in which immature neurons (2–3 weeks old) in the DG could be effectively labeled by GFP (Overstreet et al., 2004). We crossed hAPP-J20 and hAPP-I5 mice with POMC-GFP mice to generate offspring to study GFP-labeled neurons. As shown in Figure 3, GFP-labeled cells displayed typical morphology of immature neurons. Their somas were largely located in the SGZ, and the apical dendrites were short and less elaborated. We found that there was no difference in the localization of the GFP-labeled immature neurons in the DG of hAPP-J20, hAPP-I5 and control mice (Figures 3A, 3D, and 3F), suggesting that migration of newborn neurons was not affected by overexpressing either hAPP or Aβ. We then quantified the adult-born immature neurons in the DG in mice of differing age. At 1 month old, neurogenesis was quite active, and therefore dense populations of immature neurons were observed in the DG (Figure 3A). Because the neurons were tightly packed together, it was difficult to quantify them by direct counting. Considering that GFP was exclusively expressed in immature neurons in the hippocampus, we sought to quantify the immature neurons indirectly by determining GFP expression levels in the hippocampus with western blotting analysis. No difference of GFP expression levels was found in the hippocampus among hAPP-J20/POMC-GFP, hAPP-I5/POMC-GFP, and NTG/POMC-GFP mice (Figures 3B and 3C), indicating that immature neurons in the DG of hAPP-J20 and hAPP-I5 mice at 1 month of age were not affected in comparison with control mice. For 2.5-month-old mice, the number of immature neurons in the DG of hAPP-I5 mice was reduced to about 30% of control mice. In the DG of hAPP-J20 mice, however, the degree of reduction of immature neurons was much smaller (to about 70% of control mice) (Figures 3D and 3E). Direct comparison between hAPP-I5 and hAPP-J20 also revealed that there were significantly more newborn immature neurons in the DG of hAPP-J20 mice. Similar results were obtained for mice at 4.5 months old (Figures 3F and 3G). To determine whether overexpression of hAPP affects the GFP expression per se in POMC-GFP mice, we stained brain sections from NTG/POMC-GFP and hAPP/POMC-GFP mice with anti-DCX antibody. Our results showed that the GFP signal was almost completely aligned with the DCX expression in the hippocampus of either NTG/POMC-GFP or hAPP/POMC-GFP mice (Figure S2), suggesting that the reduced GFP signal in the hippocampus of hAPP/POMC-GFP mice was due to reduced neurogenesis but not reduced GFP expression.

To compare the populations of active neural progenitors, we injected 2.5-month-old hAPP-I5 and hAPP-J20 mice with BrdU and euthanized them 2 hr later. Quantification of $BrdU^+$ cells showed that the number of active neural progenitors was significantly decreased in the DG of hAPP-I5 mice compared with that in control mice (Figures 4A and 4B). However, the number of active neural progenitors in the DG of hAPP-J20 mice was slightly increased compared with that in the DG of control mice, although it did not reach statistical significance. Direct comparison revealed that there were more active neural progenitors in the DG of hAPP-J20 mice than in the DG of hAPP-I5 mice (Figures 4A and 4B).

During adult hippocampal neurogenesis, many newborn neurons died before they reached maturation. To compare the number of mature adult-born new neurons in the DG between hAPP-I5 and hAPP-J20 mice, we quantified the number of $BrdU^+/NeuN^+$ cells 28 days after the last injection of BrdU. Our results showed that there were more mature newborn neurons in the DG of hAPP-J20 mice than in hAPP-I5 mice (Figures S3A–S3E).

(D) Representative photomicrographs of GFP^+ immature neurons in the DG of 2.5-month-old hAPP-I5/POMC-GFP and hAPP-J20/POMC-GFP mice and their age-matched controls. Scale bar, 100 μm.
(E) Quantification of GFP^+ immature neurons in the DG of hAPP-I5/POMC-GFP (n = 7, 3 female and 4 male), hAPP-J20/POMC-GFP (n = 5, 3 female and 2 male), and POMC-GFP mice (n = 9, 5 female and 4 male) at 2.5 months old. $^{**}p < 0.01$, $^{***}p < 0.001$ (one-way ANOVA with Newman-Keuls post hoc test); values represent mean ± SEM.
(F) Representative photomicrographs of GFP^+ immature neurons in the DG of 4.5-month-old wild-type and mutant hAPP/POMC-GFP mice and their age-matched controls. Scale bar, 100 μm.
(G) Quantification of GFP^+ immature neurons in the DG of hAPP-I5/POMC-GFP (n = 5, 3 female and 2 male), hAPP-J20/POMC-GFP (n = 9, 5 female and 4 male), and POMC-GFP mice (n = 10) at 4.5 months old. $^{*}p < 0.05$, $^{***}p < 0.001$ (one-way ANOVA with Newman-Keuls post hoc test); values represent mean ± SEM.
See also Figure S2.

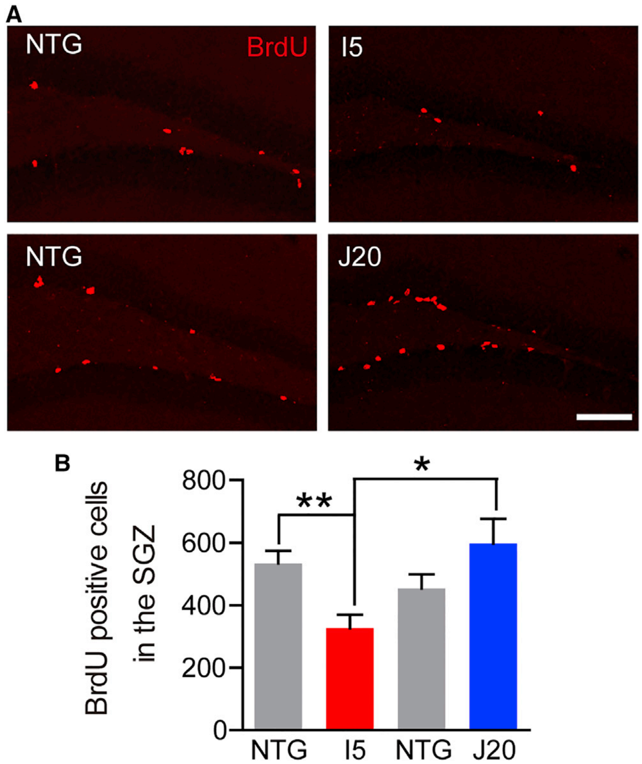

Figure 4. Neural Stem Cells Numbered Fewer in the DG of hAPP-I5 Mice Than in the DG of hAPP-J20 Mice

(A) Representative photomicrographs of immunostaining for BrdU in hAPP-I5 and hAPP-J20 mice (2.5 months old) at 2 hr after BrdU injection. Scale bar, 100 μm.

(B) Quantification of $BrdU^+$ active neural progenitor cells in the DG of hAPP-I5 (n = 5, 3 female and 2 male) and hAPP-J20 mice (n = 4, 2 female and 2 male). *p < 0.05, **p < 0.01 (one-way ANOVA with Newman-Keuls post hoc test); values represent mean ± SEM.

See also Figure S3.

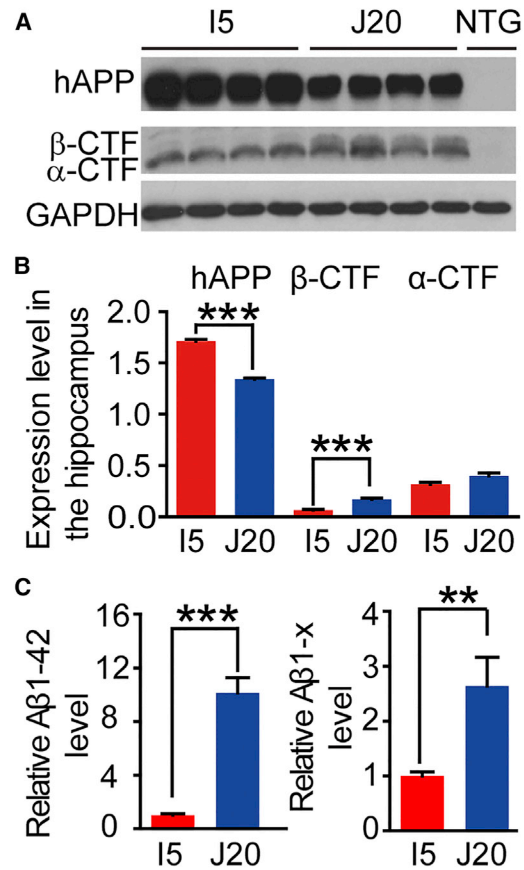

Figure 5. hAPP Processing and Aβ Levels Were Different in the Hippocampi of 2.5-Month-Old hAPP-I5 and hAPP-J20 Mice

(A) Hippocampal lysates from hAPP-I5, hAPP-J20, and non-transgenic control mice were analyzed by western blotting for detecting hAPP (6E10), β-CTF, and α-CTF (CT15). GAPDH severed as the loading control.

(B) Quantification of western blots showed significantly increased hAPP, reduced β-CTF, and similar α-CTF levels in the hippocampus of hAPP-I5 mice compared with those in the DG of hAPP-J20 mice (n = 4, 2 female and 2 male). ***p < 0.001 (unpaired t test); values represent mean ± SEM.

(C) Comparison of human Aβ1–42 and Aβ1–x levels by ELISA in the hippocampus of mice overexpressing wild-type (hAPP-I5; n = 7, 5 female and 2 male) and mutant hAPP (hAPP-J20; n = 5, 3 female and 2 male). **p < 0.01, ***p < 0.001 (unpaired t test); values represent mean ± SEM.

See also Figure S4.

Taken together, our data revealed that adult neurogenesis was suppressed in the DG of both hAPP-J20 and hAPP-I5 mice. However, it was more significantly impaired in the DG of hAPP-I5 than in the DG of hAPP-J20 mice.

hAPP Processing and Aβ Levels Were Different in the Hippocampi of hAPP-J20 and hAPP-I5 Mice

Although the mRNA levels of hAPP were quite similar between hAPP-J20 and hAPP-I5 mice, it was not clear whether this was still the case at the protein level. We therefore analyzed the expression of hAPP protein and its enzymatic fragments by western blotting. Our results revealed that the hAPP protein level was significantly higher in the hippocampus of hAPP-I5 mice than in the hippocampus of hAPP-J20 mice (Figures 5A, 5B, and S4A–S4C). However, the β-CTF (β-carboxyl terminal fragment) level was much lower in hAPP-I5 mice, while the α-CTF (α-carboxyl terminal fragment) levels were similar between hAPP-I5 and hAPP-J20 mice (Figures 5A and 5B). Furthermore, the level of sAPPβ was similar in the hippocampi of hAPP-I5 and hAPP-J20 mice (Figure S4A), but the level of sAPPα was significantly higher in the hippocampus of hAPP-I5 mice than that of hAPP-J20 mice (Figure S4B). Collectively, these data suggested that hAPP was processed differently in hAPP-I5 and hAPP-J20 mice. We also determined the levels

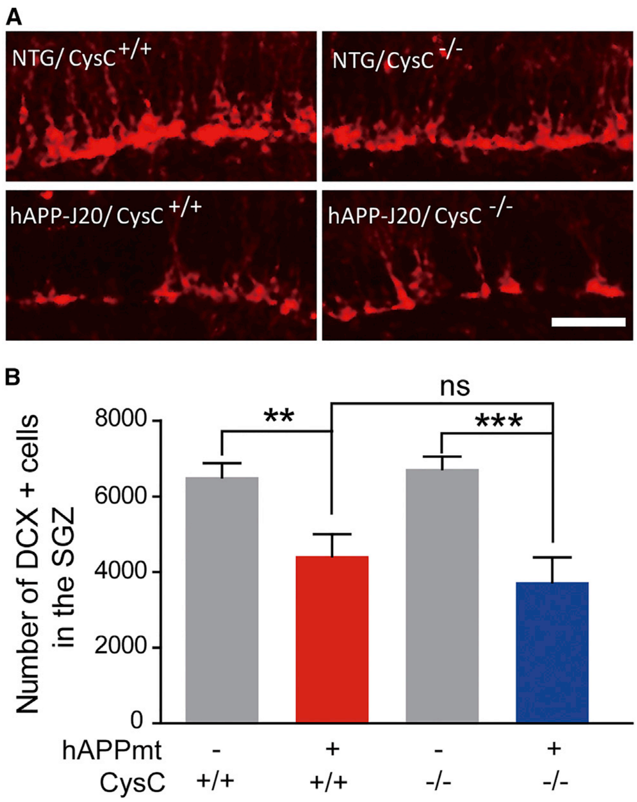

Figure 6. Reducing Aβ Levels Did Not Affect DCX+ Immature Neurons in the DG of hAPP-J20 Mice

(A) Representative photomicrographs of DCX+ immature neurons in the DG from 2.5-month-old mice of four genotypes: NTG/CysC$^{+/+}$, NTG/CysC$^{-/-}$, hAPP-J20/Cysc$^{+/+}$, and hAPP-J20/Cysc$^{-/-}$. CysC, cystatin C. Scale bar, 50 μm.

(B) Number of DCX+ cells was not changed in hAPP-J20/*CST3*$^{-/-}$ mice (n = 10, 6 female and 4 male) with lower levels of Aβ compared with hAPP-J20/*CST3*$^{+/+}$ mice (n = 9, 5 female and 4 male). ns, no significant difference. $^{**}p < 0.01$, $^{***}p < 0.001$ (one-way ANOVA with post hoc Tukey's multiple comparison test); values represent mean ± SEM.

of soluble Aβ in the hippocampus of hAPP-I5 and hAPP-J20 mice by ELISA. Consistent with previous reports (Mucke et al., 2000), levels of both total Aβ and Aβ42 were indeed much higher in hAPP-J20 mice than those in hAPP-I5 mice (Figure 5C). Western blot analysis revealed that oligo-Aβ was barely detected in the hippocampus of hAPP-I5 mice at 2.5 months of age. However, weak bands of oligo-Aβ were observed in the hippocampus of hAPP-J20 mice at 2.5 months of age (Figure S4C). These data indicated that differently processed hAPP might account for the different changes in adult hippocampal neurogenesis between hAPP-I5 and hAPP-J20 mice, and that Aβ was not the major factor impairing adult hippocampal neurogenesis.

Reducing Aβ Levels Did Not Affect DCX+ Immature Neurons in the DG of hAPP-J20 Mice

To verify our assumption that Aβ was not the major factor accounting for the impaired adult hippocampal neurogenesis, we compared the numbers of DCX+ immature neurons in the DG between hAPP-J20 mice and hAPP-J20 mice with reduced Aβ levels. We demonstrated previously that levels of both total Aβ and Aβ42 were significantly reduced (around 45% for total Aβ and 60% for Aβ42, respectively) in the hippocampus of hAPP-J20 mice after deleting cystatin C, an endogenous inhibitor of cathepsin B that truncated Aβ from the C termini (Mueller-Steiner et al., 2006; Sun et al., 2008). On the other hand, cystatin C deletion did not affect the processing of hAPP (Sun et al., 2008). Taking advantage of these findings, we analyzed the DCX+ neurons in the DG of NTG/*CST3*$^{+/+}$, hAPP-J20/*CST3*$^{+/+}$, NTG/*CST3*$^{-/-}$, and hAPP-J20/*CST3*$^{-/-}$ mice. *CST3* is the gene encoding cystatin C. We found that cystatin C deficiency did not affect the number of DCX+ neurons in the DG of NTG mice (Figures 6A and 6B). However, DCX+ neurons were much fewer in the DG of hAPP-J20/*CST3*$^{+/+}$ mice compared with NTG mice (Figures 6A and 6B). More interestingly, no difference of DCX+ neurons was observed in the DG between hAPP-J20/*CST3*$^{+/+}$ and hAPP-J20/*CST3*$^{-/-}$ mice (Figures 6A and 6B), even if the Aβ levels were significantly reduced in the latter mice. These results further suggested that Aβ was not the major factor accounting for impaired adult hippocampal neurogenesis in hAPP-J20 mice.

DISCUSSION

Our study showed that high levels of wild-type hAPP affected different stages of adult hippocampal neurogenesis. More importantly, our results suggested that Aβ was not the major factor affecting neurogenesis in the hippocampus of adult mice overexpressing hAPP.

Adult hippocampal neurogenesis has been investigated in different lines of mice overexpressing mutant hAPP (Chuang, 2010; Donovan et al., 2006; Yu et al., 2009). Surprisingly, however, studies on the effects of wild-type hAPP on adult neurogenesis have been very rare, considering that most AD patients did not express the mutant forms of APP (Soldner and Jaenisch, 2015). In an earlier study, BrdU-labeling results indicated that a high level of wild-type hAPP reduced the proliferative ability of progenitor cells and promoted the survival of newborn neurons in the DG (Naumann et al., 2010). In our present study, we used both BrdU labeling and retroviral vector expressing GFP to investigate the changes in numbers and morphological features of newborn neurons, respectively. Consistent with a previous report (Naumann et al., 2010), we found that the proliferative activity of progenitor cells in the DG of hAPP-I5 mice was decreased, as shown by BrdU labeling and MCM2 immunostaining. By crossing hAPP-I5 mice with Nestin-GFP mice (a reporter line of neural stem cells) (Mignone et al., 2004), we found that the depletion of the neural progenitor cell population was accelerated in the DG of hAPP-I5 mice (data not shown). Similarly, neural progenitor proliferation in the DG was increased in APP knockout mice (Wang et al., 2014). These data suggested that APP from both human and mouse inhibited the proliferative ability of neural progenitors in the DG. We found that the number of DCX^+ immature neurons in the DG of hAPP-I5 mice was fewer than that in nontransgenic control mice. This result was confirmed by crossing hAPP-I5 with POMC-GFP mice, in which GFP could label immature neurons in the DG with similarly aged DCX^+ neurons (Overstreet et al., 2004). Furthermore, we found not only that the number of mature newborn neurons ($BrdU^+/NeuN^+$) decreased, but also that the dendrites of newborn neurons in the DG of hAPP-I5 mice were shorter than those of control mice. These results indicated that different developmental stages of adult hippocampal neurogenesis were affected by high levels of wild-type hAPP.

Naumann et al. (2010) reported that the absolute number of $BrdU^+$ cells at 4 weeks after the last BrdU injection was similar between hAPP-I5 and control mice, which is inconsistent with our results. One possibility for this discrepancy might be the age of mice used in the studies. Six-week-old mice were used in Naumann's experiments whereas we used 10-week-old mice in our study. Neurogenesis was more active in younger mice, and therefore the effect of wild-type hAPP on neurogenesis might be counteracted partially by the active neurogenesis in younger mice. Wang et al. (2014) found that the dendritic growth of newborn neurons in the DG was significantly reduced in APP knockout mice, suggesting that both a too low and too high level of APP were detrimental to the development of newborn neurons.

Driven by the same promoter, PDGF β-chain, hAPP-I5 mice expressed wild-type hAPP and hAPP-J20 mice expressed hAPP with Swedish and Indiana mutations in neurons, respectively (Mucke et al., 2000). The expression level of hAPP mRNA was similar in the brains of hAPP-I5 and hAPP-J20 mice. However, a previous study (Mucke et al., 2000) reported that the levels of Aβ were much higher in the brain of hAPP-J20 compared with hAPP-I5 mice, which we confirm in the present study. We found that the impairment of adult hippocampal neurogenesis was more prominent in hAPP-I5 mice than that of hAPP-J20 mice, suggesting that Aβ was not the major factor accounting for the impairment of adult neurogenesis. We also found that hAPP-J20 mice expressed more oligomeric Aβ in the hippocampus in comparison with hAPP-I5 mice, further suggesting that Aβ was not a main factor in the inhibition of adult neurogenesis. In a niche presented with a high level of Aβ, the proliferation, determination, and survival of hippocampal adult-born neurons were not affected (Yetman and Jankowsky, 2013), also suggesting that Aβ was not the major culprit for the impairment of adult neurogenesis. Retroviral delivery of α-CTF into neural progenitors affected the development of newborn neurons (Morgenstern et al., 2013), further suggesting that Aβ production was not necessary to inhibit adult hippocampal neurogenesis. Our results showed that downregulating Aβ levels by crossing hAPP-J20 mice with $CST3^{-/-}$ mice did not result in changes in adult hippocampal neurogenesis, providing more direct and convincing evidence that Aβ was not responsible for impaired adult hippocampal neurogenesis in both hAPP-I5 and hAPP-J20 mice used in our study.

Although comparable levels of hAPP mRNA were detected in the brain of hAPP-I5 and hAPP-J20 mice, our western blotting analysis revealed that hAPP-I5 mice expressed significantly higher levels of hAPP protein, lower levels of β-CTF, and similar levels of α-CTF in the hippocampus and cortex compared with hAPP-J20 mice, suggesting that overexpressed hAPP but not Aβ might inhibit adult neurogenesis. Additional analysis of the fragments of hAPP revealed a higher level of sAPPα in the hippocampus of hAPP-I5 mice, but the level of sAPPβ was similar in the hippocampi of hAPP-I5 and hAPP-J20 mice, suggesting that sAPPα but not sAPPβ could also be involved in impaired adult neurogenesis in APP mice.

Because *hAPP* gene expression was driven by the PDGF β-chain promoter, hAPP could be derived from different types of neurons in both hAPP-I5 and hAPP-J20 mice. Therefore, it was unclear as to which sources of hAPP were to blame for the impaired adult neurogenesis. Recent studies showed that overexpression of hAPP exclusively in mature projection neurons in the forebrain did not affect neurogenesis in the adult hippocampus (Yetman and Jankowsky, 2013), whereas overexpression of hAPP in neural progenitor cells via retroviral delivery significantly affected the morphology and function of adult-born new neurons in the DG (Morgenstern et al., 2013), suggesting a cell-autonomous effect of APP on adult neurogenesis. However, we could not exclude the possibility that other sources of APP from either GABAergic neurons or even glial cells would affect adult neurogenesis. In fact, selective deletion of APP in GABAergic interneurons affected different processes of adult hippocampal neurogenesis (Wang et al., 2014). Further studies are warranted to dissect the definitive factor(s) affecting adult neurogenesis in hAPP-overexpressing mice.

In conclusion, our data demonstrated that different stages of adult hippocampal neurogenesis were disturbed in mice overexpressing wild-type hAPP, and Aβ was not the major factor accounting for impaired neurogenesis in the adult hippocampus of APP-overexpressing mice. However, further studies are needed to investigate the effects and mechanisms of different hAPP fragments from different resources in adult hippocampal neurogenesis.

EXPERIMENTAL PROCEDURES

Animals

hAPP-I5 mice were purchased from the Jackson Laboratory (stock #004662). hAPP-J20 mice were purchased from the JAX MMRRC (stock #034836). hAPP-I5 mice express wild-type human APP driven by PDGF β-chain promoter. hAPP-J20 mice express an hAPP minigene with the Swedish (K670N, M671L) and Indiana (V717F) mutations under the control of PDGF β-chain promoter (Mucke et al., 2000). The mRNA level of hAPP in hAPP-I5 mice was comparable with that in hAPP-J20 mice. However, the Aβ levels in hAPP-I5 mice were much lower than those in hAPP-J20 mice (Mucke et al., 2000). Both hAPP-I5 and hAPP-J20 mice lines were bred with C57BL/6J females to generate offspring for studies. Age- and sex-matched nontransgenic (NTG) mice were used as controls. POMC-GFP mice were obtained from Muming Poo (Institute of Neuroscience, Chinese Academy of Sciences), respectively. $CST3^{-/-}$ mice were provided by Dr. Anders Grubb (Department of Clinical Chemistry, Lund University Hospital). All mice were maintained on a C57BL/6J background except *CST3* genetically removed mice ($CST3^{-/-}$). $CST3^{-/-}$ mice have 57% C57BL/6J and 43% 129 background. All studies were gender balanced. Animals were housed in a pathogen-free barrier facility with a 12:12-hr light/dark cycle and ad libitum access to food and water. All experiments were approved by the Institutional Animal Care and Use Committee of Zhejiang University.

BrdU Labeling

BrdU (B5002, Sigma) was dissolved in PBS to a concentration of 10 mg/mL and the aliquots were stored at −20°C. For cell proliferation analysis, BrdU (200 mg/kg) was injected intraperitoneally once and animals were perfused 2 hr later. For cell-survival analysis, BrdU (100 mg/kg) was injected intraperitoneally twice a day at 6-hr intervals for 3 consecutive days. Mice were perfused at 28 days after the last injection. For comparing the BrdU-labeled cells between hAPP-I5 and controls, hAPP-I5 mice and their nontransgenic controls were treated together (BrdU injection, perfusion, and microtome sectioning), and immunostaining was done together. For comparison between hAPP-I5 and hAPP-J20, hAPP-I5 mice, nontransgenic controls of hAPP-I5, hAPP-J20, and nontransgenic controls of hAPP-J20 mice were treated together (BrdU injection, perfusion, and microtome sectioning), and immunostaining was done together.

Preparation and Stereotactic Injection of Retroviral Vectors Expressing GFP

Retrovirus-expressing GFP was prepared as described previously (Tashiro et al., 2006b). In brief, a murine Moloney leukemia virus-based retroviral vector (CAG-EGFP, kindly provided by Fred Gage, Salk Institute) was cotransfected with pCMV-vsv-g (envelope vector) and pCMV-gag pol into HEK293T cells with Lipofectamine 2000 (11668-019, Invitrogen). HEK293T cells were maintained in DMEM (11965, Gibco) without antibiotics before transfection. At 5 hr after plasmid transfection, culture medium was changed to DMEM with antibiotics. Culture medium was then collected 48 hr later and concentrated by ultracentrifugation. Viral pellets were dissolved in PBS and the aliquots were stored at −80°C. For labeling of adult-born new neurons, viral solution (3 μL) was delivered into the DG of 2.5-month-old mice by stereotactic injection (0.5 μL/min) bilaterally with the following coordinates (Paxinos and Franklin, 2004): anterior-posterior, −2.1 mm; medial-lateral, ±1.7 mm; and vertical, −2.0 mm. For all injections, the bregma served as the reference point.

Immunofluorescence Staining and Counting

Mice were perfused transcardially with 0.9% saline. Brains were removed immediately and immersed into 4% paraformaldehyde solution. Coronal brain sections (30 μm) were prepared with a sliding microtome (Leica). Free-floating brain sections were first blocked with blocking buffer (10% serum, 1% nonfat milk, 0.2% gelatin in PBS containing 0.5% Triton X-100) and then incubated with primary antibodies: rabbit anti-GFP (1:500 dilution; A11122, Invitrogen), goat anti-DCX (1:100 dilution; SC-8806, Santa Cruz Biotechnology), mouse anti-NeuN (1:1,000 dilution; MABN140, Millipore), mouse anti-BrdU (1:200 dilution; 11170376001, Roche), mouse anti-MCM2 (1:200 dilution; 610701, BD Biosciences), followed by incubation with appropriate secondary antibodies: donkey anti-rabbit 488 (1:250 dilution; 711-545-152, Jackson Laboratory), donkey anti-goat cy3 (1:250 dilution; 705-165-147, Jackson Laboratory), and donkey anti-mouse cy3 and 594 (1:250 dilution; 715-165-150 and 715-585-150, Jackson Laboratory). All images of dendritic structures were obtained from CAG-EGFP-injected brains stained with GFP antibody to amplify the GFP signal. For BrdU and MCM2 staining, sections were pretreated with 2 N HCl at 37°C for 30 min, washed in 0.1 M borate buffer (pH 8.5) for 10 min, then washed in TBS + Tween 20 (TBST)-Triton (10 mM Tris-HCl [pH 7.4], including 150 mM NaCl, 0.05% Tween 20, and 1% Triton X-100) for 30 min at room temperature before incubation with blocking buffer (10% serum in 0.05% TBST).

Cells in the DG were quantified blindly in every tenth serial coronal section (30 μm in thickness) through a 40× objective, throughout the rostrocaudal extent of the granule cell layer. Eight coronal sections were analyzed per mouse, and the counted numbers were then multiplied by 10 to calculate group means.

Confocal Image Analysis

For dendritic length analysis, z-series stacks of optical images were obtained at 2-μm intervals with a confocal microscope (LSM510 Meta, Zeiss). For dendritic spine density analysis, z-series stacks of optical images were obtained at 0.5-μm intervals with a confocal microscope (FV1000). Two-dimensional projections of each z series were created with ImageJ. All individual GFP-positive granule cells that had continuous dendritic trees were analyzed for total dendritic length. The total dendritic length of all individual GFP-positive granule cells was measured with ImageJ. The length of each dendritic segment was measured by tracing the center of the dendritic shaft with ImageJ. The number of spines was counted manually by ImageJ. The spine density was calculated by dividing the total number of spines by the length of the dendritic segment.

Western Blotting Analysis

Cortical and hippocampal samples were homogenized and sonicated at 4°C in RIPA buffer containing 10 mM HEPES (pH 7.4), 150 mM NaCl, 50 mM NaF, 1 mM EDTA, 1 mM DTT, 1 mM phenylmethylsulfonyl fluoride, 1 mM Na_3VO_4, 10 μg/mL leupeptin, 10 μg/mL aprotinin, and 1% SDS. Equal amounts of protein (by BCA assay) were resolved by SDS-PAGE and transferred to nitrocellulose membranes. After blocking, membranes were labeled with mouse anti-tubulin (1:5,000 dilution; KM9003, Sungene Biotech), rabbit anti-CT15 antibody (1:1,000 dilution; a kind gift of E.H. Koo, University of California, San Diego) for C-terminal fragments of APP, 6E10 (1:1,000 dilution; SIG39320, Covance) for APP and sAPPα, a mixture of 266, 21F12, and 3D6 (1:1,000 dilution; Janssen Research & Development) for oligo-Aβ, anti-APP C-terminal antibody (1:5,000 dilution; 171610, Millipore) for APP and sAPPβ, or rabbit anti-GAPDH antibody (1:5,000 dilution; 5174S, CST), and then incubated with the following secondary antibodies: horseradish peroxidase-conjugated goat anti-rabbit antibody (GAR007, LiankeBio) and goat anti-mouse antibody (GAM007, LiankeBio) of appropriate dilution ratio. Bands were visualized by enhanced chemiluminescence, and the densitometry measurements of the bands were acquired from scanned images with Quantity One software (Bio-Rad).

Quantification of Aβ

hAPP-I5 and hAPP-J20 mice (around 2.5 months old) were perfused transcardially with PBS. Brains were removed immediately and the hippocampi were dissected out and placed into liquid nitrogen. Samples were stored at −80°C until analysis. Snap-frozen hippocampi were homogenized in guanidine buffer, and soluble human Aβ peptides were measured by ELISA as described previously (Johnson-Wood et al., 1997). EIA plates (96 wells; Corning) were coated with 266 (for Aβ1–x) and 21F12 (for Aβ1–42), respectively. Biotin-3D6 was used as detection antibody. 266, 21F12, and 3D6 were provided by Janssen Research & Development. The Aβ1–42 ELISA only detects Aβ1–42, whereas Aβ1–x ELISA detects Aβ1–40, Aβ1–42, and Aβ1–43, as well as C-terminally truncated forms of Aβ containing amino acids 1–28.

Statistical Analysis

Statistical analyses were conducted with GraphPad Prism 5. Differences between two means were assessed with an unpaired two-tailed t test. Differences between three or more means were assessed by one-way ANOVA. Only values with $p < 0.05$ were accepted as significant.

SUPPLEMENTAL INFORMATION

Supplemental Information includes four figures and can be found with this article online at http://dx.doi.org/10.1016/j.stemcr.2016.08.019.

AUTHOR CONTRIBUTIONS

B.S. and H.P. conceived and designed the study; H.P., D.W., X.Z., D.Z., H.Z., Q.Q., X.H., Z.L., Y.L., T.Z., L.Z., and M.W. performed all experiments; H.P. and B.S. processed and analyzed all data; and B.S. and H.P. wrote the manuscript.

ACKNOWLEDGMENTS

We thank Fred Gage for the CAG-EGFP retroviral vector, Muming Poo for the POMC-GFP mice, Anders Grubb for the *CST3*$^{-/-}$ mice, Edward Koo for CT15 antibody, and Janssen Research & Development for antibodies 266, 21F12, and 3D6. Yanjiang Wang provided anti-APP antibody. This work was supported by grants from the Major State Basic Research Program of China (2014CB964602 to B.S.), the National Natural Science Foundation of China (91132713 to B.S.), the Zhejiang Provincial Natural Science Foundation of China (LR13H090001 to B.S.), and the Research Fund for the Doctoral Program of Higher Education of China (20110101120094 to B.S.).

Received: March 25, 2016
Revised: August 30, 2016
Accepted: August 31, 2016
Published: September 29, 2016

REFERENCES

Boekhoorn, K., Joels, M., and Lucassen, P.J. (2006). Increased proliferation reflects glial and vascular-associated changes, but not neurogenesis in the presenile Alzheimer hippocampus. Neurobiol. Dis. *24*, 1–14.

Bond, A.M., Ming, G.-L., and Song, H. (2015). Adult mammalian neural stem cells and neurogenesis: five decades later. Cell Stem Cell *17*, 385–395.

Christian, K.M., Song, H., and Ming, G.-L. (2014). Functions and dysfunctions of adult hippocampal neurogenesis. Annu. Rev. Neurosci. *37*, 243–262.

Chuang, T.T. (2010). Neurogenesis in mouse models of Alzheimer's disease. Biochim. Biophys. Acta *1802*, 872–880.

Clelland, C., Choi, M., Romberg, C., Clemenson, G., Fragniere, A., Tyers, P., Jessberger, S., Saksida, L., Barker, R., and Gage, F. (2009). A functional role for adult hippocampal neurogenesis in spatial pattern separation. Science *325*, 210–213.

Deng, W., Aimone, J.B., and Gage, F.H. (2010). New neurons and new memories: how does adult hippocampal neurogenesis affect learning and memory? Nat. Rev. Neurosci. *11*, 339–350.

Donovan, M.H., Yazdani, U., Norris, R.D., Games, D., German, D.C., and Eisch, A.J. (2006). Decreased adult hippocampal neurogenesis in the PDAPP mouse model of Alzheimer's disease. J. Comp. Neurol. *495*, 70–83.

Ehninger, D., and Kempermann, G. (2008). Neurogenesis in the adult hippocampus. Cell Tissue Res. *331*, 243–250.

Epis, R., Gardoni, F., Marcello, E., Genazzani, A., Canonico, P.L., and Di Luca, M. (2010). Searching for new animal models of Alzheimer's disease. Eur. J. Pharmacol. *626*, 57–63.

Eriksson, P.S., Perfilieva, E., Björk-Eriksson, T., Alborn, A.-M., Nordborg, C., Peterson, D.A., and Gage, F.H. (1998). Neurogenesis in the adult human hippocampus. Nat. Med. *4*, 1313–1317.

Ge, S., Yang, C.-h., Hsu, K.-s., Ming, G.-L., and Song, H. (2007). A critical period for enhanced synaptic plasticity in newly generated neurons of the adult brain. Neuron *54*, 559–566.

Haughey, N.J., Nath, A., Chan, S.L., Borchard, A., Rao, M.S., and Mattson, M.P. (2002). Disruption of neurogenesis by amyloid β-peptide, and perturbed neural progenitor cell homeostasis, in models of Alzheimer's disease. J. Neurochem. *83*, 1509–1524.

Jin, K., Peel, A.L., Mao, X.O., Xie, L., Cottrell, B.A., Henshall, D.C., and Greenberg, D.A. (2004). Increased hippocampal neurogenesis in Alzheimer's disease. Proc. Natl. Acad. Sci. USA *101*, 343–347.

Johnson-Wood, K., Lee, M., Motter, R., Hu, K., Gordon, G., Barbour, R., Khan, K., Gordon, M., Tan, H., and Games, D. (1997). Amyloid precursor protein processing and Aβ42 deposition in a transgenic mouse model of Alzheimer disease. Proc. Natl. Acad. Sci. USA *94*, 1550–1555.

Kang, E., Wen, Z., Song, H., Christian, K.M., and Ming, G.-L. (2016). Adult neurogenesis and psychiatric disorders. Cold Spring Harb. Perspect. Biol. *8*, a019026.

Li, B., Yamamori, H., Tatebayashi, Y., Shafit-Zagardo, B., Tanimukai, H., Chen, S., Iqbal, K., and Grundke-Iqbal, I. (2008). Failure of neuronal maturation in Alzheimer disease dentate gyrus. J. Neuropathol. Exp. Neurol. *67*, 78–84.

Lledo, P.-M., Alonso, M., and Grubb, M.S. (2006). Adult neurogenesis and functional plasticity in neuronal circuits. Nat. Rev. Neurosci. *7*, 179–193.

Marlatt, M.W., Potter, M.C., Bayer, T.A., van Praag, H., and Lucassen, P.J. (2013). Prolonged running, not fluoxetine treatment, increases neurogenesis, but does not alter neuropathology, in the 3xTg mouse model of Alzheimer's disease. Curr. Top. Behav. Neurosci. *15*, 313–340.

Mignone, J.L., Kukekov, V., Chiang, A.S., Steindler, D., and Enikolopov, G. (2004). Neural stem and progenitor cells in nestin-GFP transgenic mice. J. Comp. Neurol. *469*, 311–324.

Morgenstern, N.A., Giacomini, D., Lombardi, G., Castaño, E.M., and Schinder, A.F. (2013). Delayed dendritic development in newly generated dentate granule cells by cell-autonomous expression of the amyloid precursor protein. Mol. Cell Neurosci. *56*, 298–306.

Mucke, L., Masliah, E., Yu, G.-Q., Mallory, M., Rockenstein, E.M., Tatsuno, G., Hu, K., Kholodenko, D., Johnson-Wood, K., and McConlogue, L. (2000). High-level neuronal expression of Aβ1-42 in wild-type human amyloid protein precursor transgenic mice: synaptotoxicity without plaque formation. J. Neurosci. *20*, 4050–4058.

Mueller-Steiner, S., Zhou, Y., Arai, H., Roberson, E.D., Sun, B., Chen, J., Wang, X., Yu, G., Esposito, L., and Mucke, L. (2006). Antiamyloidogenic and neuroprotective functions of cathepsin B: implications for Alzheimer's disease. Neuron *51*, 703–714.

Naumann, N., Alpár, A., Ueberham, U., Arendt, T., and Gärtner, U. (2010). Transgenic expression of human wild-type amyloid precursor protein decreases neurogenesis in the adult hippocampus. Hippocampus *20*, 971–979.

Nilsson, M., Perfilieva, E., Johansson, U., Orwar, O., and Eriksson, P.S. (1999). Enriched environment increases neurogenesis in the adult rat dentate gyrus and improves spatial memory. J. Neurobiol. *39*, 569–578.

Overstreet, L.S., Hentges, S.T., Bumaschny, V.F., De Souza, F.S., Smart, J.L., Santangelo, A.M., Low, M.J., Westbrook, G.L., and Rubinstein, M. (2004). A transgenic marker for newly born granule cells in dentate gyrus. J. Neurosci. *24*, 3251–3259.

Paxinos, G., and Franklin, K.B. (2004). The Mouse Brain in Stereotaxic Coordinates (Gulf Professional Publishing).

Restivo, L., Niibori, Y., Mercaldo, V., Josselyn, S.A., and Frankland, P.W. (2015). Development of adult-generated cell connectivity with excitatory and inhibitory cell populations in the hippocampus. J. Neurosci. *35*, 10600–10612.

Richetin, K., Leclerc, C., Toni, N., Gallopin, T., Pech, S., Roybon, L., and Rampon, C. (2015). Genetic manipulation of adult-born hippocampal neurons rescues memory in a mouse model of Alzheimer's disease. Brain *138*, 440–455.

Sahay, A., Scobie, K.N., Hill, A.S., O'Carroll, C.M., Kheirbek, M.A., Burghardt, N.S., Fenton, A.A., Dranovsky, A., and Hen, R. (2011a). Increasing adult hippocampal neurogenesis is sufficient to improve pattern separation. Nature *472*, 466–470.

Sahay, A., Wilson, D.A., and Hen, R. (2011b). Pattern separation: a common function for new neurons in hippocampus and olfactory bulb. Neuron *70*, 582–588.

Serrano-Pozo, A., Frosch, M.P., Masliah, E., and Hyman, B.T. (2011). Neuropathological alterations in Alzheimer disease. Cold Spring Harb. Perspect. Med. *1*, a006189.

Shors, T.J., Miesegaes, G., Beylin, A., Zhao, M., Rydel, T., and Gould, E. (2001). Neurogenesis in the adult is involved in the formation of trace memories. Nature *410*, 372–376.

Soldner, F., and Jaenisch, R. (2015). Dissecting risk haplotypes in sporadic Alzheimer's disease. Cell Stem Cell *16*, 341–342.

Spalding, K.L., Bergmann, O., Alkass, K., Bernard, S., Salehpour, M., Huttner, H.B., Boström, E., Westerlund, I., Vial, C., and Buchholz, B.A. (2013). Dynamics of hippocampal neurogenesis in adult humans. Cell *153*, 1219–1227.

Sultan, S., Li, L., Moss, J., Petrelli, F., Cassé, F., Gebara, E., Lopatar, J., Pfrieger, F.W., Bezzi, P., and Bischofberger, J. (2015). Synaptic integration of adult-born hippocampal neurons is locally controlled by astrocytes. Neuron *88*, 957–972.

Sun, B., Zhou, Y., Halabisky, B., Lo, I., Cho, S.-H., Mueller-Steiner, S., Devidze, N., Wang, X., Grubb, A., and Gan, L. (2008). Cystatin C-cathepsin B axis regulates amyloid beta levels and associated neuronal deficits in an animal model of Alzheimer's disease. Neuron *60*, 247–257.

Sun, B., Halabisky, B., Zhou, Y., Palop, J.J., Yu, G., Mucke, L., and Gan, L. (2009). Imbalance between GABAergic and glutamatergic transmission impairs adult neurogenesis in an animal model of Alzheimer's disease. Cell Stem Cell *5*, 624–633.

Tashiro, A., Sandler, V.M., Toni, N., Zhao, C., and Gage, F.H. (2006a). NMDA-receptor-mediated, cell-specific integration of new neurons in adult dentate gyrus. Nature *442*, 929–933.

Tashiro, A., Zhao, C., and Gage, F.H. (2006b). Retrovirus-mediated single-cell gene knockout technique in adult newborn neurons in vivo. Nat. Protoc. *1*, 3049–3055.

Valero, J., Espana, J., Parra-Damas, A., Martin, E., Rodriguez-Alvarez, J., and Saura, C.A. (2011). Short-term environmental enrichment rescues adult neurogenesis and memory deficits in APP(Sw,Ind) transgenic mice. PLoS One *6*, e16832.

van Praag, H., Kempermann, G., and Gage, F.H. (1999). Running increases cell proliferation and neurogenesis in the adult mouse dentate gyrus. Nat. Neurosci. *2*, 266–270.

van Praag, H., Schinder, A.F., Christie, B.R., Toni, N., Palmer, T.D., and Gage, F.H. (2002). Functional neurogenesis in the adult hippocampus. Nature *415*, 1030–1034.

Wang, B., Wang, Z., Sun, L., Yang, L., Li, H., Cole, A.L., Rodriguez-Rivera, J., Lu, H.-C., and Zheng, H. (2014). The amyloid precursor protein controls adult hippocampal neurogenesis through GABAergic interneurons. J. Neurosci. *34*, 13314–13325.

Winner, B., Kohl, Z., and Gage, F.H. (2011). Neurodegenerative disease and adult neurogenesis. Eur. J. Neurosci. *33*, 1139–1151.

Yetman, M.J., and Jankowsky, J.L. (2013). Wild-type neural progenitors divide and differentiate normally in an amyloid-rich environment. J. Neurosci. *33*, 17335–17341.

Yu, Y., He, J., Zhang, Y., Luo, H., Zhu, S., Yang, Y., Zhao, T., Wu, J., Huang, Y., and Kong, J. (2009). Increased hippocampal neurogenesis in the progressive stage of Alzheimer's disease phenotype in an APP/PS1 double transgenic mouse model. Hippocampus *19*, 1247–1253.

Yun, J., Koike, H., Ibi, D., Toth, E., Mizoguchi, H., Nitta, A., Yoneyama, M., Ogita, K., Yoneda, Y., and Nabeshima, T. (2010). Chronic restraint stress impairs neurogenesis and hippocampus-dependent fear memory in mice: possible involvement of a brain-specific transcription factor Npas4. J. Neurochem. *114*, 1840–1851.

Zhao, C., Teng, E.M., Summers, R.G., Ming, G.-L., and Gage, F.H. (2006). Distinct morphological stages of dentate granule neuron maturation in the adult mouse hippocampus. J. Neurosci. *26*, 3–11.

Zhao, C., Deng, W., and Gage, F.H. (2008). Mechanisms and functional implications of adult neurogenesis. Cell *132*, 645–660.